

Immobilization of a bubble in water by nanoelectrolysis

Zoubida Hammadi, Laurent Lapena, Roger Morin, and Juan Olives^{a)}

CINaM-CNRS Aix-Marseille Univ., Campus de Luminy, case 913, 13288 Marseille Cedex 9, France

(Dated: 7 February 2017)

A surprising phenomenon is presented: a bubble, produced from water electrolysis, is immobilized in the liquid (as if the Archimedes' buoyant force were annihilated). This is achieved using a nanoelectrode (1 nm to 1 μm of curvature radius at the apex) and an alternating electric potential with adapted values of amplitude and frequency. A simple model based on "nanoelectrolysis" (i.e., nanolocalization of the production of H_2 and O_2 molecules at the apex of the nanoelectrode) and an "open bubble" (i.e., exchanging H_2 and O_2 molecules with the solution) explains most of the observations.

Microbubbles have many applications: medicine (contrast agents,¹ gas embolotherapy,² blood clot lysis³) or nuclear industry.⁴ Questions about their stability remain topical.⁵ H_2/O_2 microbubbles are easily generated by water electrolysis and their production is controlled by the electric potential. Recently, H_2 microbubbles have been used to rotate a microobject.⁶ Droplets may also be controlled by electrolysis.⁷ Many applications will result from a more effective control on the microbubbles and, especially, on each individual microbubble. Our preceding paper⁸ showed a first example of such control: the nanolocalization of the production of microbubbles at a unique point of a tip-shaped electrode, under precise values of the amplitude and the frequency of the alternating potential. This phenomenon will be called nanoelectrolysis (for bubble production). The relation between microbubble production and current intensity will be given in a forthcoming paper. The present paper describes a surprising phenomenon, which represents an example of control of a single microbubble: the immobilization of a bubble in the liquid (as if the Archimedes' buoyant force were annihilated).

The experimental procedure is described in Ref. 8. Water electrolysis is performed using an aqueous solution containing 10^{-4} mol/L of H_2SO_4 and a periodic alternating applied potential, here of rectangular shape:⁹ $V(t) = V_m$ for $0 < t < T/2$, $V(t) = -V_m$ for $T/2 < t < T$ (T is the period and $\nu = 1/T$ the frequency). The amplitudes V_m typically range from 2 V to 30 V. Two Pt electrodes are used and one of the two electrodes—called nanoelectrode—is tip-shaped, with a curvature radius, at the apex of the electrode, ranging from 1 nm to 1 μm . In the previous paper,⁸ we showed that, for definite values of the amplitude and the frequency of the potential, the microbubbles are produced at a single point, the apex of the nanoelectrode. We start in such conditions, so that microbubbles are successively generated at the apex of the electrode and then naturally go up towards the air-solution surface, owing to the Archimedes' buoyant force. Let us now describe the observed phenomenon. Immediately after the production of a microbubble, if we rapidly

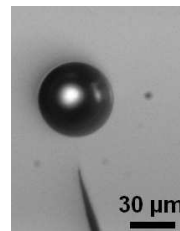


FIG. 1. Microbubble immobilized in the solution, above the apex of the nanoelectrode (potential $V_m = 3$ V, $\nu = 1000$ Hz).

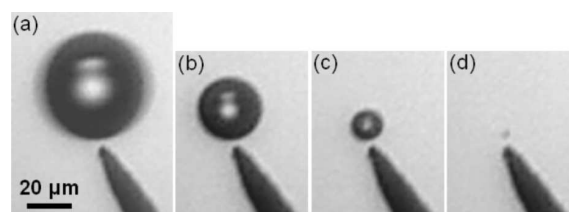


FIG. 2. Immobilized bubble, slowly decreasing with time ($V_m = 3.43$ V, $\nu = 1000$ Hz): $t = 0$ (a), $t = 2$ min 6 s (b), $t = 3$ min 55 s (c) and $t = 4$ min 33 s (d). Same scale for all the images.

increase the frequency (generally, up to at least 500 or 1000 Hz; and then, maintaining constant the frequency; V_m remaining always constant), then the microbubble remains immobile in the solution,¹⁰ at some distance from the electrode and nearly at the vertical of the apex of the electrode (Fig. 1). In addition, this configuration is stable, since the bubble remains at the vertical of the apex of the electrode and at the same distance from the electrode, when this electrode is moved in any direction with respect to the solution (see the video¹¹). This immobilization is observed during various minutes or hours (at constant amplitude V_m and frequency). The diameters D' of the immobilized bubbles typically range from some μm to 400 μm . This diameter may remain constant, in some cases, but very frequently decreases with time, as shown in Fig. 2, till the (optical) disappearance of the microbubble. As the diameter D' decreases with time (Fig. 3), we observe that the distance r_C between

^{a)} Electronic mail: olives@cinam.univ-mrs.fr

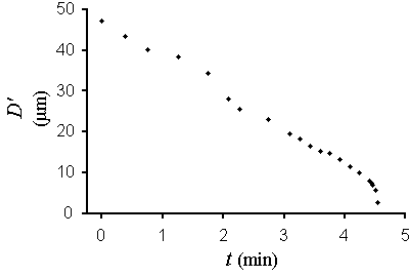


FIG. 3. Diameter D' of the bubble versus time t , for the experiment shown in Fig. 2.

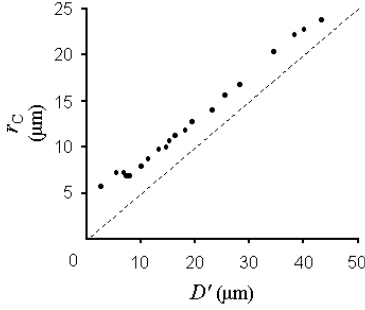


FIG. 4. Relation between r_C (distance between the center of the bubble and the apex of the electrode) and D' (diameter of the bubble), for the experiment shown in Fig. 2. The dashed line represents the equation $r_C = D'/2$.

the center of the bubble and the apex of the electrode also decreases (Fig. 4). The evolution of the diameter decreasing rate dD'/dt as a function of the diameter is shown in Fig. 5, for three different experiments.

In order to understand such a strange phenomenon, we first note that the bubble cannot be considered as a closed system (i.e., with no exchange of matter with the solution) and its immobilization as a balance between the Archimedes' buoyant force and a new force. Indeed, such a (downward) force should increase with the distance between the bubble and the apex of the electrode (in order to explain the stability of this equilibrium, shown in the video¹¹), which seems unrealistic. Our explanation is then based on a bubble considered as an open system, exchanging matter with the solution through its (immobile) surface. In this case, the new forces which might counterbalance the Archimedes' one are the flux of momentum entering the bubble and the hydrodynamic forces. However, these forces are intimately associated with the fields of the pressures, velocities, and densities and the determination of these fields is a very complex coupled problem (involving hydrodynamics, diffusion, and mass fluxes kinetics at the bubble-solution interface). This problem is not treated here and will be investigated in the future by using computer simulations. As an approximation, hydrodynamics equations (concerning the pressures and

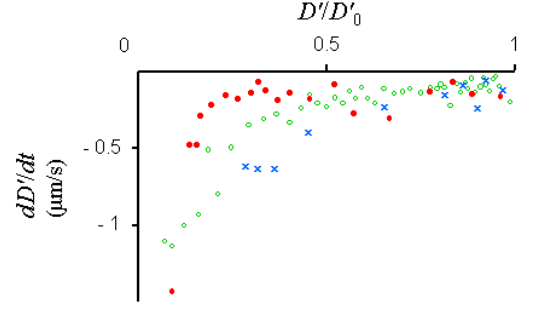


FIG. 5. Diameter decreasing rate dD'/dt versus D'/D'_0 (D'_0 = initial diameter at $t = 0$) for the experiment shown in Fig. 2 (solid circles), another experiment with $V_m = 27.5$ V, $\nu = 500$ Hz, and $D'_0 = 63$ μm (crosses), and a third experiment with $V_m = 21$ V, $\nu = 500$ Hz, and $D'_0 = 260$ μm (empty circles).

the velocities) may be separated and, in the following, we show that a simplified model based on the mass balance, diffusion, and interface fluxes equations may explain—at least qualitatively—most of the above observations.

In our previous paper,⁸ we showed that the bubble production is nanolocalized (at the apex of the nano-electrode) when the potential v (applied to the dielectric layer, at the electrode-electrolyte interface) reaches a threshold value v_0 . Similarly, we expect that the chemical reactions of electrolysis will be also nanolocalized for a (lower) threshold value v'_0 . According to our model,⁸ this implies that, in the potential amplitude-frequency plane, the domain for the nanolocalization of the electrolysis reactions is shifted toward higher frequencies, with respect to that for the nanolocalization of bubble production. Thus, after the increase in frequency needed for the immobilization of the bubble, the new present amplitude-frequency values correspond to conditions of no bubble production,⁸ but we here assume that they correspond to nanolocalization conditions for the electrolysis reactions: i.e., these reactions still occur and are nanolocalized at the apex of the electrode, although the rate of production of H_2 and O_2 molecules is not enough to generate bubbles. These molecules, produced at the apex of the electrode, thus remain and diffuse in the solution, without generating any bubble. In our model, the immobilized bubble is considered as an open system, which may exchange H_2 and O_2 molecules with the solution through its surface. The whole system (solution and bubble) is considered in a steady state.

The bubble contains H_2 and O_2 molecules, and the general model for a bubble containing these two components is given in the supplementary material.¹¹ This model shows that, in the steady state (and for not too small diameters), the bubble contains nearly the same number of moles of H_2 and O_2 (although the production of O_2 molecules is lower than that of H_2 , and the solubility of O_2 is higher than that of H_2 ; this is due to the low diffusion coefficient of O_2).¹¹ In the following, for

the sake of simplicity, we present the model for a bubble containing only one component, e.g., H_2 . Let us use the subscript $i = 1$ to denote the H_2 component in the solution and the subscripts $i = 2, 3, \dots$ for the other components of the solution (such as O_2 , H_2O , H^+ , ...). The diffusion flux of H_2 is given by Fick's law:

$$j_1 = \rho_1(v_1 - v) = -D_1 \text{grad} \rho_1 \quad (1)$$

(ρ_i and v_i are, respectively, the volume mass density and the velocity of the component i ; v is the barycentric or convection velocity defined by $\rho v = \rho_1 v_1 + \rho_2 v_2 + \dots$, ρ being the mass density of the solution; D_1 is the diffusion coefficient $= 4.6 \times 10^{-9} \text{ m}^2/\text{s}$ for H_2 in water at 20°C). In the solution, the H_2 mass balance equation

$$\frac{\partial \rho_1}{\partial t} + \text{div}(\rho_1 v_1) = \dot{m}_1 \delta \quad (2)$$

(\dot{m}_1 is the mass production per unit time at the apex of the electrode, which is considered as the origin point; δ is the Dirac measure—in space—at this origin point; \dot{m}_1 , averaged on a period, is considered constant in this simple model) leads to

$$-D_1 \Delta \rho_1 + v \cdot \text{grad} \rho_1 = \dot{m}_1 \delta \quad (3)$$

(with the help of Eq. (1), $\frac{\partial \rho_1}{\partial t} = 0$ —steady state—and $\text{div} v = 0$ —incompressibility).

At each point of the surface S of the bubble, the flux of H_2 entering the bubble is

$$j_S = \rho_1(v_1 - v_S) \cdot n = \rho(v - v_S) \cdot n \quad (4)$$

(assuming only exchanges of H_2 between the bubble and the solution; n is the unit vector normal to S , oriented towards the interior of the bubble; v_S is the normal velocity of the surface, parallel to n ; obviously, $v_S = 0$ for an immobile bubble), which gives, according to Eq. (1)

$$-D_1 \partial_n \rho_1 = (1 - \frac{\rho_1}{\rho}) j_S \approx j_S. \quad (5)$$

We assume that the exchange of H_2 between the solution and the bubble is controlled by the simple kinetic law

$$j_S = K(\rho_1 - H p'), \quad (6)$$

where $p' = p_a + \frac{2\gamma}{R'}$ is the pressure in the bubble (p_a the atmospheric pressure, γ the surface tension, $R' = D'/2$ the bubble radius), H the Henry's constant, and K the mass transfer coefficient ($\gamma = 7.28 \times 10^{-2} \text{ N/m}$, the water–air value at 20°C ; $H = 1.62 \times 10^{-3} \text{ kg}/(\text{m}^3 \text{ atm})$ for H_2 in water at 20°C (Ref. 12)).

As a simple model, we use the ρ_1 field produced only by diffusion (i.e., satisfying to Eq. (3) with $v = 0$), without taking into account the presence of the bubble (i.e., the condition Eq. (5))

$$\rho_1 = \frac{\dot{m}_1}{4\pi D_1} \frac{1}{r}, \quad (7)$$

where r is the distance to the origin point O (which is the apex of the electrode). If r_0 denotes the distance at

which $\rho_1(r_0) = H p_a$ (corresponding to the equilibrium of H_2 between the solution and H_2 gas at the atmospheric pressure), Eq. (6) takes the form

$$j_S = K H p_a \left(\frac{r_0}{r} - \left(1 + \frac{2\tilde{\gamma}}{R'}\right) \right), \quad (8)$$

where $\tilde{\gamma} = \frac{\gamma}{p_a}$. A simple calculation then gives the variation of the mass m' of the bubble

$$\frac{dm'}{dt} = \int_S j_S da = j_S(r_C) a_S, \quad (9)$$

where da is the area measure, $a_S = 4\pi R'^2$ the area of S , and $j_S(r_C)$ the value of j_S (from Eq. (8)) at $r = r_C$ (and for the radius R' ; C is the center of the bubble, r_C the distance OC). Eq. (9) expresses that the mass or the diameter of a bubble (the center of which is) situated at $r_C = r_0/(1 + \frac{2\tilde{\gamma}}{R'})$ remains constant, whereas that of a bubble situated at $r_C > r_0/(1 + \frac{2\tilde{\gamma}}{R'})$ (respectively, at $r_C < r_0/(1 + \frac{2\tilde{\gamma}}{R'})$) decreases (respectively, increases).

Note that, although Eq. (5) is not strictly satisfied with the approximate expression Eq. (7), it is however “qualitatively” satisfied if r_T (i.e., the distance OT) is equal to $r_0/(1 + \frac{2\tilde{\gamma}}{R'})$, T being a point of S such that OT is tangent to S (see Fig. 6). Indeed, at T , we have $\partial_n \rho_1 = n \cdot \text{grad} \rho_1 = 0$ (since $\text{grad} \rho_1$ is directed from T to O , according to Eq. (7)) and $j_S = 0$ (since $r_T = r_0/(1 + \frac{2\tilde{\gamma}}{R'})$), so that Eq. (5) is satisfied at T , i.e., on the horizontal circle Γ of S generated by these points T . Let us denote S_- the part of S situated below the circle Γ , and S_+ that situated above Γ . At any point M of S_- , we have $\partial_n \rho_1 = n \cdot \text{grad} \rho_1 < 0$ ($\text{grad} \rho_1$ being directed from M to O) and $j_S > 0$ (since $r_M < r_0/(1 + \frac{2\tilde{\gamma}}{R'})$), so that the two members of Eq. (5) have the same positive sign. In a similar way, the two members of this equation have the same negative sign, if M belongs to S_+ . With respect to the sign of the two members of Eq. (5), we may then consider that this equation is “qualitatively”

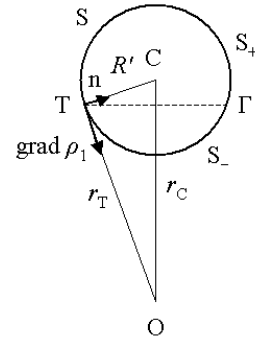


FIG. 6. Geometrical configuration. O is the apex of the nanoelectrode, C the center of the bubble, S its surface, T a point of S such that OT is tangent to S , Γ the horizontal circle generated by these points T , S_- the part of S situated below Γ , and S_+ that situated above Γ .

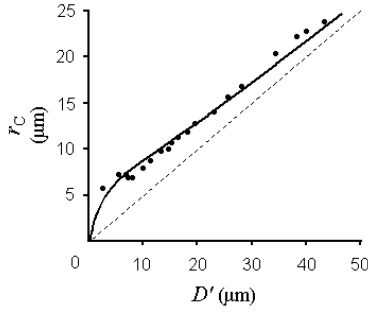


FIG. 7. Relation between r_C (distance between the center of the bubble and the apex of the electrode) and $D' = 2R'$ (diameter of the bubble) as expressed by Eq. (10), with $r_0 = 9.5 \mu\text{m}$ (continuous line), for comparison with the experimental points of Fig. 4 (dots). The dashed line represents the equation $r_C = D'/2$.

satisfied. Thus, H_2 molecules enter the bubble through S_- ($j_S > 0$) and leave the bubble through S_+ ($j_S < 0$). Note that the main assumption is here the approximate expression Eq. (7) (which does not take into account either the velocity field or the presence of the bubble).

A first consequence of this situation is that $r_C > r_0/(1 + \frac{2\tilde{\gamma}}{R'})$ (since $r_C > r_T$) which, as noted above, indicates that the diameter of the bubble decreases with time. This is consistent with the experiments, since bubbles decreasing in diameter with time are the most frequently observed. Another consequence is the following relation between r_C and R'

$$r_C = \sqrt{R'^2 + \left(\frac{r_0}{1 + \frac{2\tilde{\gamma}}{R'}}\right)^2} \quad (10)$$

(according to the value of r_T ; see Fig. 6), which is in agreement with the observations: see Fig. 7, drawn with $r_0 = 9.5 \mu\text{m}$, for comparison with the experimental points of Fig. 4. Note that, according to Eq. (7) and $\rho_1(r_0) = H p_a$, this value of r_0 corresponds to $\dot{m}_1/M_1 = 4\pi D_1 r_0 H p_a/M_1 = 4.4 \times 10^{-13} \text{ mol H}_2/\text{s}$ (produced at the apex of the nanoelectrode; M_1 being the molar mass of H_2) and an effective electrolysis current intensity—averaged on the half period during which the nanoelectrode is cathode— $I_e = 2 \times 2N_A q_e \dot{m}_1/M_1 = 0.17 \mu\text{A}$ (N_A the Avogadro constant, q_e the elementary charge). These values of \dot{m}_1/M_1 and I_e are divided by 2 in the general model with both H_2 and O_2 components.¹¹

From the relation $m' = \frac{M_1}{RT} p_a (1 + \frac{2\tilde{\gamma}}{R'}) \frac{4\pi}{3} R'^3$ between R' and m' , and Eq. (9), one easily obtains

$$\frac{dR'}{dt} = K \bar{H} R T \frac{\frac{r_0}{r_C} - (1 + \frac{2\tilde{\gamma}}{R'})}{1 + \frac{4\tilde{\gamma}}{3R'}}, \quad (11)$$

R being the gas constant, T the temperature, and $\bar{H} = H/M_1$. If R' is not too small, this expression (with r_C given by Eq. (10)) leads to a relatively constant value of dR'/dt as R' decreases. This may explain the relatively

constant value of dD'/dt during a large first part of each experiment (see Figs. 3 and 5). In addition, for large values of R' , i.e., also large values of r_C (according to Eq. (10)), Eq. (11) leads to a “universal” limit value of dR'/dt

$$\left(\frac{dR'}{dt}\right)_{\text{lim}} = -K \bar{H} R T, \quad (12)$$

which seems to be in agreement with the observations. Indeed, for large values of D' , we observe that dD'/dt has nearly the same value, of about $-0.15 \mu\text{m/s}$, in very different experiments (see Fig. 5). By applying Eq. (12), this value leads to a mass transfer coefficient $K \approx 4 \mu\text{m/s}$ (at 20°C) which may be considered as a qualitatively acceptable value: indeed, in the literature, the value of this coefficient is not well known and ranges from some $\mu\text{m/s}$ to some hundreds of $\mu\text{m/s}$.^{5,13,14} Note that the decreasing behavior of dD'/dt for the small diameter values (Fig. 5) is not explained with this model. We currently try to improve the present model and to automate the experimental procedure in order to completely determine the conditions in which this surprising immobilization phenomenon occurs.

The presented experimental setup, i.e., the immobilized bubble and the nanoelectrode microdisplacement actuator, constitutes a point probe of acoustical pressure,¹⁵ as well as a promising tool for sizing microbubbles.¹⁶

We thank Serge Mensah and Younes Achaoui for helpful discussions and acknowledge the financial support from “Smart US” ANR agreement.

¹S. H. Bloch, M. Wan, P. A. Dayton, and K. W. Ferrara, *Appl. Phys. Lett.* **84**, 631 (2004).

²A. Qamar, Z. Z. Wong, J. B. Fowlkes, and J. L. Bull, *Appl. Phys. Lett.* **96**, 143702 (2010).

³C. Acconcia, B. Y. C. Leung, K. Hynnenen, and D. E. Goertz, *Appl. Phys. Lett.* **103**, 053701 (2013).

⁴T. J. Kim, V. S. Yughay, S. T. Hwang, B. H. Kim, J. H. Park, and C. S. Choi, *J. Ind. Engin. Chem.* **6**, 395 (2000).

⁵K. Aoki, H. Toda, J. Yamamoto, J. Chen, and T. Nishiumi, *J. Electroanal. Chem.* **668**, 83 (2012).

⁶N. Li and J. Hu, *Appl. Phys. Lett.* **103**, 124101 (2013).

⁷C. Poulain, A. Dugué, A. Durieux, N. Sadeghi, and J. Duplat, *Appl. Phys. Lett.* **107**, 064101 (2015).

⁸Z. Hammadi, R. Morin, and J. Olives, *Appl. Phys. Lett.* **103**, 223106 (2013).

⁹A potential of sinusoidal shape may also be used.

¹⁰If the increase in frequency is not sufficiently rapid, the bubble will continue to go up and will not be immobilized.

¹¹See, as supplementary material, (1) video showing the immobilization of a bubble (experiment of Fig. 1) and the stability of this configuration when the electrode is moved (recording speed 100 images/s, reading speed 10 images/s), and (2) general model for a bubble containing H_2 and O_2 .

¹²R. Sander, *Atmos. Chem. Phys.* **15**, 4399 (2015).

¹³N. Itoh and A. M. Sathe, *J. Membrane Sci.* **137**, 251 (1997).

¹⁴H. Matsushima, D. Kiuchi, and Y. Fukunaka, *Electrochim. Acta* **54**, 5858 (2009).

¹⁵G. Renaud, J. G. Bosch, A. F. W. Van Der Steen, and N. De Jong, *Ultrasound Med. Biol.* **40**, 1282 (2014).

¹⁶K. Czarniecki, D. Fouan, Y. Achaoui, and S. Mensah, *J. Sound Vibration* **356**, 48 (2015).